RESEARCH ARTICLE





First-year Acacia seedlings are anisohydric "water-spenders" but differ in their rates of water use

Scott T. Cory

William K. Smith

Abstract

T. Michael Anderson

Department of Biology, Wake Forest University, 1834 Wake Forest Road, Winston-Salem, NC 27106, USA

Correspondence

Scott T. Cory, Department of Biology, Wake Forest University, 1834 Wake Forest Road, Winston-Salem, NC 27106, USA. Email: coryst15@wfu.edu

Premise: First-year seedlings (FYS) of tree species may be a critical demographic bottleneck in semi-arid, seasonally dry ecosystems such as savannas. Given the highly variable water availability and potentially strong FYS-grass competition for water, FYS water-use strategies may play a crucial role in FYS establishment in savannas and, ultimately, in tree-grass competition and coexistence.

Methods: We examined drought responses in FYS of two tree species that are dominant on opposite ends of an aridity gradient in Serengeti, Acacia (=Vachellia) tortilis and A. robusta. In a glasshouse experiment, gas exchange and whole-plant hydraulic conductance (K_{plant}) were measured as soil water potential (Ψ_{soil}) declined. Trajectory of the $\Psi_{\text{leaf}}/\Psi_{\text{soil}}$ relationship during drought elucidated the degree of iso/anisohydry.

Results: Both species were strongly anisohydric "water-spenders," allowing rapid wet-season C gain after pulses of moisture availability. Despite being equally vulnerable to declines in K_{plant} under severe drought, they differed in their rates of water use. Acacia tortilis, which occurs in the more arid regions, initially had greater K_{max} , transpiration (E), and photosynthesis (A_{net}) than A. robusta.

Conclusions: This work demonstrates an important mechanism of FYS establishment in savannas: Rather than investing in drought tolerance, savanna FYS maximize gas exchange during wet periods at the expense of desiccation during dry seasons. FYS establishment appears dependent on high C uptake during the pulses of water availability that characterize habitats dominated by these species. This study increases our understanding of species-scale plant ecophysiology and ecosystem-scale patterns of tree-grass coexistence.

KEYWORDS

Acacia, drought, first-year seedling, hydraulic conductance, hydraulic vulnerability, iso/anisohydry continuum, savanna, Serengeti, tree-grass competition, Vachellia

Savannas are characterized by a continuous grass canopy with a spatially heterogeneous tree cover. Understanding the factors that generate and maintain this tree-grass coexistence has long been of interest (e.g., reviews by Scholes and Archer, 1997; Sankaran et al., 2005). Precipitation and its effects on soil moisture and grass productivity are considered primary drivers enabling this coexistence, although studies have also found support for the role of herbivory (Midgley et al., 2010), fire (Hoffmann et al., 2012; Holdo et al., 2014),

and soil characteristics (Rietkerk et al., 1997; Sankaran et al., 2008; Holdo et al., 2020). Numerous studies have also suggested that first-year seedlings (hereafter, FYS) are a demographic bottleneck for savanna tree species (Chidumayo, 2013; Anderson et al., 2015; Morrison et al., 2019). Thus, survival of FYS may play a critical role in maintaining the structure of savannas, yet the ecophysiological mechanisms that shape the mortality of FYS, and ultimately, tree-grass coexistence, are poorly understood.

This is an open access article under the terms of the Creative Commons Attribution-NonCommercial License, which permits use, distribution and reproduction in any medium, provided the original work is properly cited and is not used for commercial purposes.

© 2022 The Authors. American Journal of Botany published by Wiley Periodicals LLC on behalf of Botanical Society of America.

A newly emerging savanna tree seedling may experience strong limitations to growth and survival beneath the grass overstory, possibly due to both sunlight and soil water limitations. In seasonally dry savannas, highly variable water availability across seasons may strongly influence FYS-grass competition for soil water and accompanying nutrients (Chesson et al., 2004; Cramer et al., 2007). For example, in eastern Africa, productivity of perennial C4 grasses is highest during the wet season (circa November-May; Anderson et al., 2008), creating potentially strong sunlight limitations for FYS beneath the canopy during these periods. FYS not only must escape the grass canopy to avoid light limitations during the wet season, they must simultaneously compete with grasses for soil water from the same soil horizon (February et al., 2013; Ketter and Holdo, 2018). Savanna grasses are substantial water "spenders" that rapidly deplete soil moisture after a rainfall event, particularly within the top layers of soil due to their extensive, shallow root system (Williams et al., 1998). Experimentally removing grasses has been shown to increase Acacia seedling establishment (Cramer et al., 2007; Ward and Esler, 2011; Morrison et al., 2019). During the dry season, these drought-deciduous FYS may drop their leaves, and soil moisture remains low until the subsequent wet season (Xu et al., 2015). The result is a relatively short window of adequate sunlight and soil water after pulses of precipitation during which FYS must maximize carbon gain to ensure survival.

In addition to seasonality and considerable stochasticity of water availability across seasons, precipitation also varies across space in many savanna ecosystems. For example, in the Serengeti ecosystem, mean annual precipitation (MAP) ranges from ~500 mm in the southeastern Serengeti to >1200 mm in the northwestern region (McNaughton, 1985; Anderson et al., 2008). This substantially greater precipitation in the northwest supports higher primary productivity of grasses, creating strong tree-grass competition, particularly during the wet season, and therefore greater risk of FYS mortality (Morrison et al., 2019). In contrast, rainfall is more uniformly distributed across seasons in the northwest, with a greater proportion of the MAP falling during the dry season (McNaughton, 1985; Anderson et al., 2008). This interaction between the annual amount, seasonality, and stochasticity of precipitation creates pulses of resource availability and grass productivity, generating strong FYS-grass competition for soil water and sunlight (Chesson et al., 2004; Dwyer et al., 2010).

Given the highly variable water availability and strong competition for soil water in the Serengeti, the role of wateruse strategies and the vulnerability of whole-plant hydraulic pathways during drought could be a key mechanism affecting FYS survival (e.g., Johnson et al., 2011). This whole-plant hydraulic pathway ($K_{\rm plant}$) reflects xylem function (transport efficiency and vulnerability to embolism), stomatal sensitivity to declining water status (iso/anisohydry), resilience of non-xylem pathways in leaves (i.e., "outside-xylem" pathways of Scoffoni et al., 2017), and

even the hydraulic conductance of soil to supply water to roots. For example, their limited rooting volume subjects FYS to lower and more variable soil water potentials ($\Psi_{\rm soil}$) compared to larger, deeply rooted plants (McDowell et al., 2008). This exposure to extreme $\Psi_{\rm soil}$, combined with their limited capacity for carbohydrate and water storage, leaves FYS highly vulnerable to tissue desiccation and xylem embolism during drought (Grossnickle, 2012). Thus, maintaining functional hydraulic pathways is critical for maximizing gas exchange and for avoiding lethal tissue desiccation.

Generally, stomatal closure is a key mechanism by which plants control their water status and avoid the negative effects of drought. A common approach to describing these wateruse strategies is the spectrum of stomatal sensitivity to declining water potentials—the so-called iso/anisohydry continuum (Tardieu and Simonneau, 1998; McDowell et al., 2008; Martínez-Vilalta et al., 2014; Hochberg et al., 2018). On one end of this spectrum, isohydric species maintain water status (i.e., Ψ_{leaf}) by tightly regulating stomatal conductance (g_s) as xylem tension rises. Stomata close before water status drops below a critical threshold of Ψ_{leaf} that would lead to cavitation, yielding a higher hydraulic safety margin (McDowell et al., 2008; Martínez-Vilalta and Garcia-Forner, 2017; Fu and Meinzer, 2018). But, under strong competition for water with grasses during pulses of water availability, FYS might benefit from sustaining gas exchange despite high xylem tensions. This anisohydric strategy of a "water-spender" maximizes C gain during brief periods of water availability, but at the expense of potential hydraulic failure as soil moisture declines. Even though anisohydric species often have lower hydraulic vulnerability, they also have greater risk of desiccation because they operate with lower hydraulic safety margins (Martínez-Vilalta et al., 2014; Fu and Meinzer, 2018).

Theory states that, in the absence of rooting zone partitioning (Kambatuku et al., 2013; Ward et al., 2013), as reported between grasses and FYS in some African savannas (Ketter and Holdo, 2018), plants should maximize their utilization of precipitation pulses by maintaining high hydraulic conductance during droughts (Schwinning and Ehleringer, 2001). The ability to continue water transport and gas exchange would be particularly advantageous during the dry season due to a substantially greater incidence of sunlight after grass die-back, but critically low plant water potentials in this scenario would lead to catastrophic desiccation of aboveground tissues and/or resprouting when precipitation returns. This effect is likely to be compounded in high disturbance environments, such as those with frequent fire, in which dry season tissues are likely to be lost to fire until the following wet season.

Understanding these possible relationships for FYS would contribute to understanding the mechanisms governing FYS-grass coexistence in savannas and possibly FYS establishment and mortality elsewhere (Brodersen et al., 2019). Here, we investigated stomatal behavior and hydraulic traits in FYS of two coexisting tree species that are

dominant on opposite ends of an aridity gradient in the Serengeti: Acacia (=Vachellia) tortilis, which is abundant in more arid regions, and A. robusta, which is abundant in higher rainfall regions. Stomatal sensitivity to declining soil moisture and hydraulic vulnerability were examined by measuring gas exchange and whole-plant hydraulic conductance ($K_{\rm plant}$) throughout a drought experiment. We hypothesized that both species would demonstrate relatively anisohydric behavior, but that A. tortilis would sustain $K_{\rm plant}$ into more severe drought (=lower hydraulic vulnerability) than A. robusta would.

MATERIALS AND METHODS

We investigated stomatal responses to drought and hydraulic vulnerability by repeatedly measuring gas exchange and water potentials throughout a drought experiment in a greenhouse. Subsequently, we conducted an accompanying study to validate the accuracy of in situ soil water potential ($\Psi_{\rm soil}$) measurements. We also measured $\Psi_{\rm soil}$ in the field and analyzed the distribution of each species at seven long-term sites across the Serengeti.

Plant material and growth conditions

The experiment was conducted in a glasshouse facing south-southwest that was maintained at ~30°C. Seeds of Acacia (=Vachellia, family Fabaceae) tortilis (Forssk.) and A. robusta (Burch.) were collected across Serengeti National Park in Tanzania and transported to Wake Forest University. Seeds were collected opportunistically from multiple individuals at eight sites that are part of a broader study on tree dynamics in the Serengeti (Holdo et al., 2020). The seeds were scarified using sandpaper to remove a small portion of the seed coat and were then sown in cylindrical pots (40 cm tall, 10 cm diameter). To replicate the waterholding capacity of clay-rich soils in Serengeti, we used a growing medium with 12/5/3 (v/v/v) of Metro-Mix 360 Professional Growing Mix (Sun Gro Horticulture, Agawam, MA, USA), Turface Mound & Plate All-Purpose Clay (PROFILE Products, Buffalo Grove, IL, USA), and Quikrete Premium Play Sand (Quikrete, Atlanta, GA, USA), respectively. Seedlings (10 individuals of each species) were kept well watered for the first 74 days after sowing, then water was withheld for the remainder of the experiment. Measurements began on day 71 and continued until all leaves on a particular plant had dropped or until leaf water potential (Ψ_{leaf}) was less than -7 MPa (ending on day 168).

Gas exchange and hydraulic conductance

We measured whole-plant hydraulic conductance ($K_{\rm plant}$) using an evaporative flux method. $K_{\rm plant}$ was calculated using the formula of Sack et al. (2002):

$$K_{\text{plant}} = \frac{E}{\Psi_{\text{soil}} - \Psi_{\text{leaf}}}$$

In this application of Ohm's Law analogy for water transport in plants (Nobel, 2009), hydraulic conductance ($K_{\rm plant}$) is the flux of water on a leaf-area basis, given the water potential gradient across the plant. Thus, each measurement of $K_{\rm plant}$ required simultaneous measurements of steady-state transpiration (E), leaf water potential ($\Psi_{\rm leaf}$), and soil water potential ($\Psi_{\rm soil}$).

Soil water potential was measured with Teros 21 sensors (METER Group, Pullman, WA, USA) buried in every pot at a depth of 23 cm (Appendix S1). Transpiration and photosynthesis were measured with an LI-6400 fitted with an LED light source (6400-02B, Li-Cor, Lincoln, NE, USA). Chamber conditions were maintained at CO_2 concentrations of 405 ± 5 ppm and $2000 \, \mu \text{mol·m}^{-2} \cdot \text{s}^{-1}$ PPFD. Gas exchange was measured on one to four pinnae from a fully expanded bipinnately compound leaf. Leaf tissue did not entirely fill the 6-cm² chamber, so the leaf area was determined by scanning each sample, then removing artifacts in Adobe (San Jose, CA, USA) Photoshop 19.1.7. Leaf area was then determined using the LeafArea package in R (Katabuchi, 2015).

Leaf temperature during gas exchange measurements was calculated using an energy balance approach. First, chamber temperature was measured using a Type E thermocouple that was wired underneath the chamber gasket. We used boundary layer conductance values from the BLC Lookup Table (Li-Cor) after performing a sensitivity analysis, which showed that the table values were appropriate for our samples. Immediately after gas exchange measurements, Ψ_{leaf} of the same leaf as gas exchange measurements was measured (Appendix S1) using a Scholander-type pressure chamber fitted with an Almond compression gasket for short petioles (PMS Instrument Co., Albany, OR, USA).

Measurements were taken on 17 days between day 71 and 168 of the experiment. After the initial measurements when plants were well watered, plants were not measured if their soil water potential had not decreased adequately. On average, each *A. tortilis* was measured eight times, and *A. robusta* was measured 11 times.

Water potential curves

The trajectory of the relationship between Ψ_{leaf} and Ψ_{soil} was used to assess stomatal sensitivity to declining water status (iso/anisohydry). As soil moisture declines, the relationship between Ψ_{leaf} and Ψ_{soil} is often nonlinear and can be described as three phases (Meinzer et al., 2016; Fu and Meinzer, 2018). Following the procedures of Knipfer et al. (2020), we used a piecewise linear regression (PLR) approach to estimate the boundaries between Phases I and II and Phases II and III. First, we visually estimated the breakpoint between phases and used these as starting values.

We then iteratively searched values of Ψ_{soil} that minimized residual mean squared error, which provided the bounds for ordinary linear regression (Crawley, 2007).

Hydraulic vulnerability curves

Hydraulic conductance data throughout the drought experiment were used to calculate the percentage loss of conductance (PLC) using the formula:

PLC =
$$100 \times \frac{(K_{\text{max}} - K_{\text{plant}})}{K_{\text{max}}}$$
,

where $K_{\rm plant}$ values are a series of hydraulic conductance measurements throughout the experiment and $K_{\rm max}$ is each individual plant's maximum $K_{\rm plant}$ under ideal conditions (which we defined as $\Psi_{\rm leaf} > -0.2$ MPa).

Vulnerability curves were constructed by plotting PLC as a function of Ψ_{leaf} then calculating the water potential required to induce a 50 and 88% loss in hydraulic conductance (P_{50} and P_{88} , respectively). We performed this analysis with the R package FitPLC (Duursma and Choat, 2017). First, starting values for P_x (the Ψ_{leaf} at x percent loss of hydraulic conductance) and S_x (the slope of the curve) were estimated from a linearized sigmoidal-exponential model using linear regression. These starting values were then used to fit a Weibull model with the formula $K/K_{\text{max}} = (1 - x/100)^p$, where $p = (P/P_x)^{P_x S_x/V}$, $V = (x - 100)\log (1 - x/100)$, and P is a range of Ψ_{leaf} values.

The model was fit for each species, using individuals as the random effect. Conductance declined rapidly within a narrow range of Ψ_{leaf} near the inflection point at P_{50} . Thus, the Weibull function was weighted more heavily near values of P_{50} (Nolf et al., 2015) using a power function, Weight = $|50 - \text{PLC}|^{1.2}$, which improved the quality of the Weibull fit (and therefore, statistical power), but did not significantly alter the P_x estimates themselves. Confidence intervals of the estimated parameters were calculated using bootstrapping (Duursma and Choat, 2017).

Leaf area estimation

A common approach to assess whole-plant hydraulics is to measure the flux of water through the entire plant (e.g., sap flow or mass balance), then standardize K by the sapwood area or the whole-plant leaf area (Yang and Tyree, 1994; Tsuda and Tyree, 1997; Venturas et al., 2017). Because gas exchange and Ψ_{leaf} were measured on individual leaves rather than the entire plant, we expressed E (and therefore, K) in terms of leaf area inside the Li-Cor chamber rather than whole-plant leaf area. Regardless of the units of K, PLC was expressed as a percentage of each individual's K_{max} when water potential was still high.

However, comparison of K_{plant} can potentially be confounded by differences in size, total leaf area, the degree of drought deciduousness, or the ratio of total leaf area to sapwood area. Previous work from our group has shown that these species have equivalent leaf area. In a prior experiment with these same two species (Rugemalila et al., 2020), we quantified the total projected leaf area (PLA), which is the total one-sided leaf area of the entire plant. Experimental conditions during the previous experiment (e.g., size of pots, glasshouse temperature, sun exposure) were nearly identical to the present study, and seedlings were similar in age (measured at day 51 in the previous experiment; onset of drought in the present experiment was on day 71). Briefly, we used a subsample of leaves to estimate the average projected area per leaf, which we then multiplied by the total number of leaves to give the total leaf area of the plant. In full sunlight, the mean PLA \pm SE was 48.51 ± 5.50 for A. robusta and $44.87 \pm 10.74 \text{ cm}^2$ for A. tortilis (n = 9 and 10, respectively). There was no significant difference in PLA between the species (t = 1.1373, df = 11.4463, P = 0.2787), indicating that differences in evaporative surface area would not confound our interpretation of K_{plant} in the present study.

Validation of Ψ_{soil} measurements

Our calculation of K_{plant} requires accurate measurement of Ψ_{soil} , which is difficult to measure in situ, particularly at extremely low Ψ_{soil} because K_{soil} can decline by orders of magnitude during soil dry-down. Thus, after the initial experiment above, we performed an additional experiment to validate the accuracy of our Ψ_{soil} sensors by comparing Ψ_{soil} measurements with predawn Ψ_{plant} . Theory suggests that in the absence of capacitance and nighttime transpiration, plant water status should equilibrate with the highest Ψ_{soil} that is available to the plant (Donovan et al., 2001). Ψ_{leaf} and Ψ_{stem} of bagged, nontranspiring plants have been used in lieu of direct measurements of Ψ at the soil-root interface (Tsuda and Tyree, 1997). To verify that our Ψ_{soil} sensors were equivalent to predawn Ψ_{leaf} (i.e., that our Ψ_{soil} sensors reflect Ψ that is actually available to the plant), we set up 11 pots with the same Teros 21 sensors, using the same soil and growing conditions as before. All pots had a sensor at the same 23-cm depth, and six of the 11 pots had additional sensors at 10- and 35-cm depths (data not shown).

Seedlings in this validation experiment were kept well watered for 126 days before water was withheld. At ~5-day intervals after water was withheld (ending on day 171), we measured predawn $\Psi_{\rm leaf}$ for comparison to $\Psi_{\rm soil}$ sensor readings. To avoid any potential effects of nighttime transpiration, we covered the entire seedling (plus a moist paper towel) in a plastic bag on the day before predawn $\Psi_{\rm leaf}$ measurements. Due to a spider mite outbreak in the glasshouse, data were included from only seven plants (107 measurements total).

Species distributions and field Ψ_{soil}

To understand the relationship between the spatial distributions of Acacia species and temporal patterns of soil moisture availability, we examined field measurements of $\Psi_{\rm soil}$ and abundance of each species at seven long-term sites across the Serengeti rainfall gradient (e.g., Anderson et al., 2015). We expected that $\Psi_{\rm soil}$ would decline more quickly in sites where A. tortilis is more abundant, which would suggest that rapid utilization of pulsed resource availability is particularly adaptive for A. tortilis.

At each study site, we selected ~10 representative rainfall events during 2015–2019 that saturated the soil and were not immediately followed by another rainfall event, allowing $\Psi_{\rm soil}$ to decline monotonically. $\Psi_{\rm soil}$ was measured with Teros 21 sensors buried at a depth of 10 cm in soils that were representative of the site. After a typical rainfall event, $\Psi_{\rm soil}$ was >–10 kPa then declined over several days or until the next rainfall event. We defined "dry-down days" as the number of days after a rainfall event for $\Psi_{\rm soil}$ to decline to –204 kPa, which is the mean $\Psi_{\rm soil}$ where $\Psi_{\rm leaf}$ begins to decline (Θ_1 from our WP curves, Figure 3).

At the same seven sites where $\Psi_{\rm soil}$ was measured, abundance of adult trees >5 cm DBH and >2 m in height of both species was recorded in $1000\,{\rm m}^2$ plots annually since 2010 (e.g., Anderson et al., 2015; Morrison et al., 2016; Rugemalila et al., 2016). We used species abundance data from our 2018 surveys and plotted the density of each species (number per $1000\,{\rm m}^2$) as a function of the dry-down days (Appendix S2).

Statistical analyses

All analyses were performed in R (R Core Team, 2018). E and $K_{\rm max}$ were log-transformed for statistical analyses. A two-sample t-test was used to test for differences in E, $\Psi_{\rm leaf}$ and $K_{\rm max}$ between species, and data are expressed as means \pm SEs. For vulnerability curves, the standard errors of P_x cannot be used for traditional statistical inference because these confidence intervals are often asymmetric. Thus, 95% confidence intervals of P_x and S_x were compared between species and were considered not significantly different if the confidence intervals overlapped (Duursma and Choat, 2017).

RESULTS

Species distributions and field Ψ_{soil}

The site-level means of dry-down days ranged from 7 to 13 days across the seven study sites. As we predicted, the density of *A. tortilis* was positively and *A. robusta* negatively related to the number of dry-down days across the Serengeti (Appendix S2).

Ψ_{soil} validation

Our validation study showed that the difference between Ψ_{soil} and predawn Ψ_{leaf} was negligible, particularly when Ψ_{soil} and $\Psi_{\text{leaf_predawn}}$ were \geq -0.2 MPa (Ψ_{soil} - $\Psi_{\text{leaf_predawn}}$ = 0.088 \pm 0.008 MPa, mean \pm SE), meaning that our Ψ_{soil} sensor readings were sufficiently accurate to use in calculations of K_{plant} . Across the entire range of Ψ_{soil} (0 to -2.11 MPa), the slope was 0.918, and R^2 = 0.6322 (Appendix S3).

Pre-drought gas exchange

Soil water potential remained >-0.015 MPa during the first 74 days after sowing (Figure 1A). At the beginning of the drought experiment, when Ψ_{soil} was still high (>-0.2 MPa), there were significant differences in water-use strategies between the species. Stomatal conductance (g_s) was initially ~50% higher in A. tortilis (Figure 1C), and transpiration (E) was also greater in A. tortilis (6.922 ± 0.632) than A. robusta $(4.364 \pm 0.231 \text{ mmol m}^{-2} \text{ s}^{-1}; F_{1,103} = 16.4, P = 9.835 \times 10^{-5};$ Figure 2A). Despite having ~59% greater water loss through transpiration, A. tortilis also had higher Ψ_{leaf} than A. robusta and -1.47 ± 0.044 MPa, (-1.18 ± 0.060) respectively; $F_{1,103} = 16.3$, $P = 1.053 \times 10^{-4}$; Figure 2B). During this initial period of the drought experiment, K_{max} (the maximum wholeplant hydraulic conductance under ideal conditions) was 80% higher for A. tortilis than A. robusta (9.716 ± 1.598 and $5.403 \pm 0.489 \text{ mmol m}^{-2} \text{ s}^{-1} \text{ MPa}^{-1}$, respectively; $F_{1,18} = 10.1$, $P = 5.219 \times 10^{-3}$; Figure 2C). Similar to E (Figure 2A), A_{net} was ~77% greater for A. tortilis than A. robusta (20.10 ± 1.26) and $11.39 \pm 0.55 \,\mu\text{mol m}^{-2} \,\text{s}^{-1}$, respectively; $F_{1.103} = 43.9$, P = 1.618×10^{-9} ; Figure 2D).

Drought responses

Due to its greater transpiration, $\Psi_{\rm soil}$ declined more rapidly for *A. tortilis* than for *A. robusta* (Figure 1A) during the drought experiment. Similarly, $\Psi_{\rm leaf}$ also declined more rapidly for *A. tortilis* (Figure 1B), reaching –5 MPa ~20 days earlier than *A. robusta*. After water was withheld, $g_{\rm s}$ of *A. tortilis* declined 74% within 1 week, from 0.4061 ± 0.1006 on day 75 to 0.1028 ± 0.0163 mol m⁻² s⁻¹ on day 82 (Figure 1C), whereas $g_{\rm s}$ and $A_{\rm net}$ in *A. robusta* declined more gradually throughout the drought (Figure 1C,D).

Water potential curves

When $\Psi_{\rm soil}$ was still high at the beginning of the drought (Phase I, Figure 3), $\Psi_{\rm leaf}$ varied largely independently of $\Psi_{\rm soil}$, likely due to day-to-day differences in vapor pressure deficit and/or irradiance (Hochberg et al., 2018; Kannenberg et al., 2021). Our PLR model identified the transition from Phase I to Phase II (Θ_1) at -0.185 for *A. robusta* and -0.223 MPa for *A. tortilis* (Figure 3). While soil drying

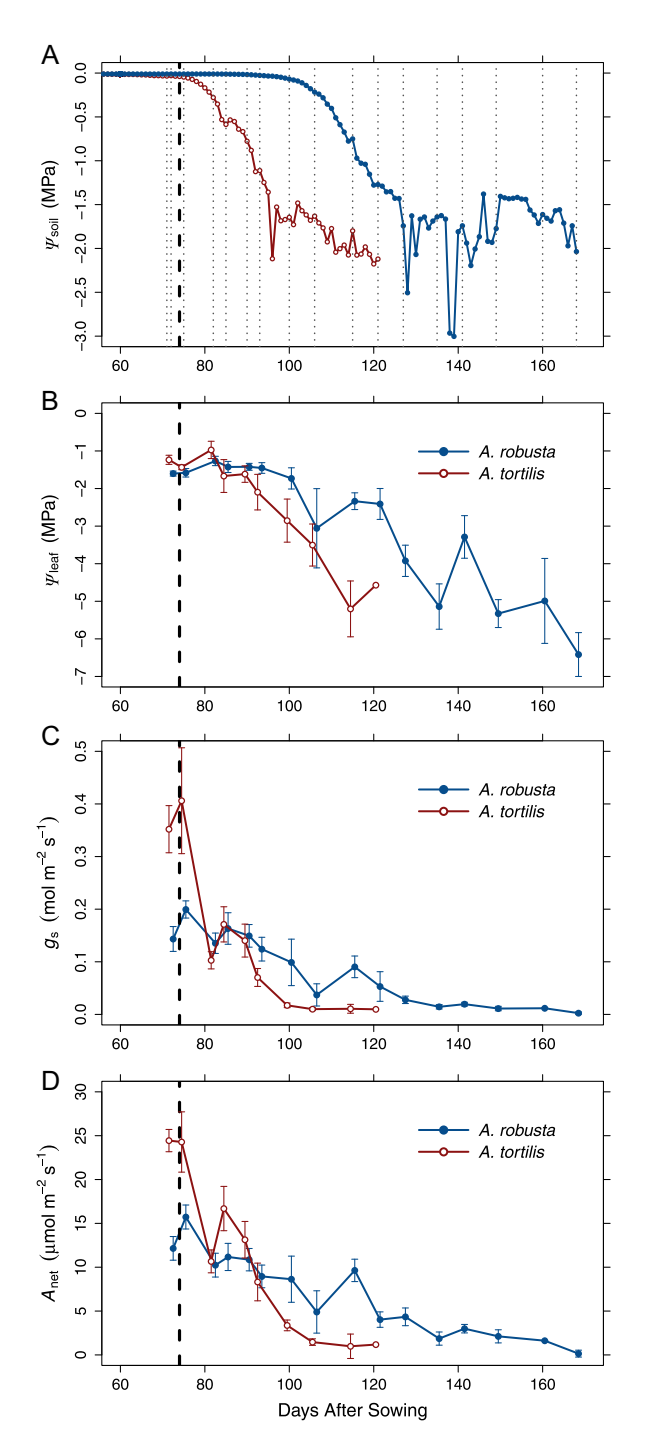


FIGURE 1 Declines in water status and gas exchange through the course of the drought experiment. Plants were well watered for 74 days after sowing, then water was withheld (thick dashed vertical line at day 74) until all leaves had dropped or until Ψ_{leaf} was < -7 MPa. (A) Soil water potential (Ψ_{soil}) remained high until water was withheld, then declined more rapidly for *Acacia tortilis* than *A. robusta*. Dotted vertical lines represent the 17 different days that (B) leaf water potential (Ψ_{leaf}) and gas exchange were measured. (C) Stomatal conductance (g_s) and (D) photosynthesis (A_{net}) was initially ~50% higher in *A. tortilis*, but declined more rapidly. Points in A are means of 10 Ψ_{soil} sensors per species. Points and error bars in B–D are means and standard errors of 3 to 10 plants per species, as some individuals were not measured on a particular day if its Ψ_{soil} had not decreased adequately since the previous measurement.

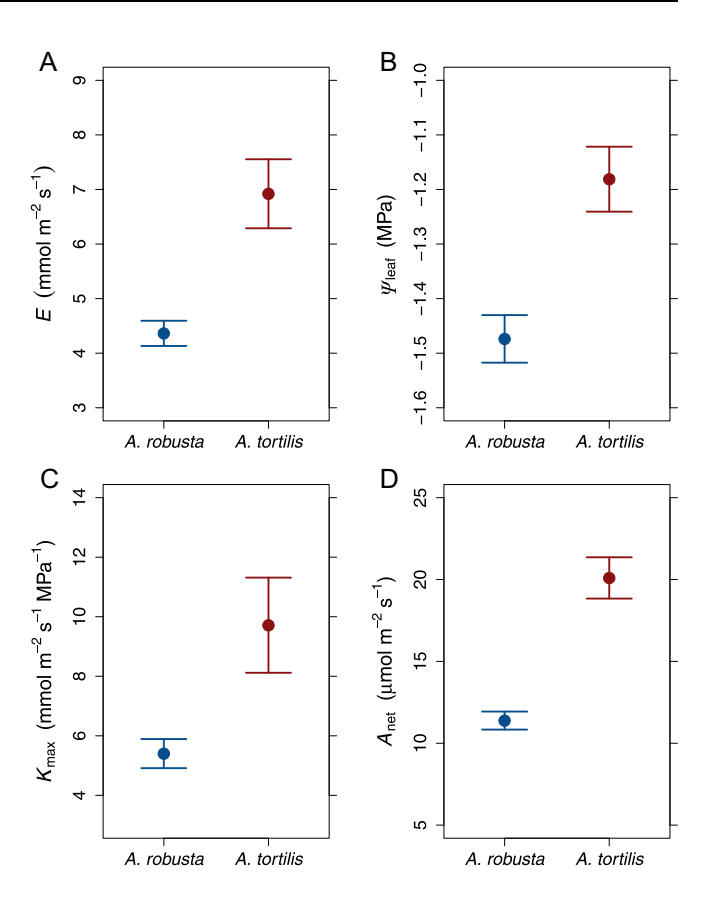


FIGURE 2 Differences between *Acacia robusta* and *A. tortilis* in gas exchange and hydraulic traits at the onset of the drought experiment when $\Psi_{\rm soil} > -0.2$ MPa. (A) *A. tortilis* had higher transpiration (*E*) yet remained at higher leaf water potential ($\Psi_{\rm leaf}$) than *A. robusta* (B). Under these well-watered conditions, *A. tortilis* had greater (C) maximum hydraulic conductance ($K_{\rm max}$) and (D) net photosynthesis ($A_{\rm net}$). Points are the means and standard errors of 10 plants per species for C. Points in A, B, D are means and standard errors of measurements where $\Psi_{\rm soil} > -0.2$ MPa (*A. tortilis*: n = 40 and *A. robusta*: n = 65).

progressed during Phase II, $\Psi_{\rm leaf}$ declined more rapidly than $\Psi_{\rm soil}$. The result is that the gradient of $\Psi_{\rm soil}$ – $\Psi_{\rm leaf}$ increased as $\Psi_{\rm soil}$ decreased, indicating a lack of stomatal regulation at these moderate levels of drought. During Phase II, the $\Psi_{\rm leaf}$ $\Psi_{\rm soil}$ relationship was y=1.834x-1.432 for A. robusta and y=1.492x-1.144 for A. tortilis. Beyond Θ_2 (at –2.004 and –2.043 for A. robusta and A. tortilis, respectively), the relationship between $\Psi_{\rm leaf}$ and $\Psi_{\rm soil}$ was weak in Phase III, suggesting that desiccation and/or xylem embolism were the primary limitation to $K_{\rm plant}$ and gas exchange.

Vulnerability curves

Despite major differences between the species in gas exchange and K_{max} when soil moisture was relatively high, we found no differences in their hydraulic vulnerability during drought (Figure 4). *Acacia tortilis* had a slightly lower estimate of P_{88} , although this difference was

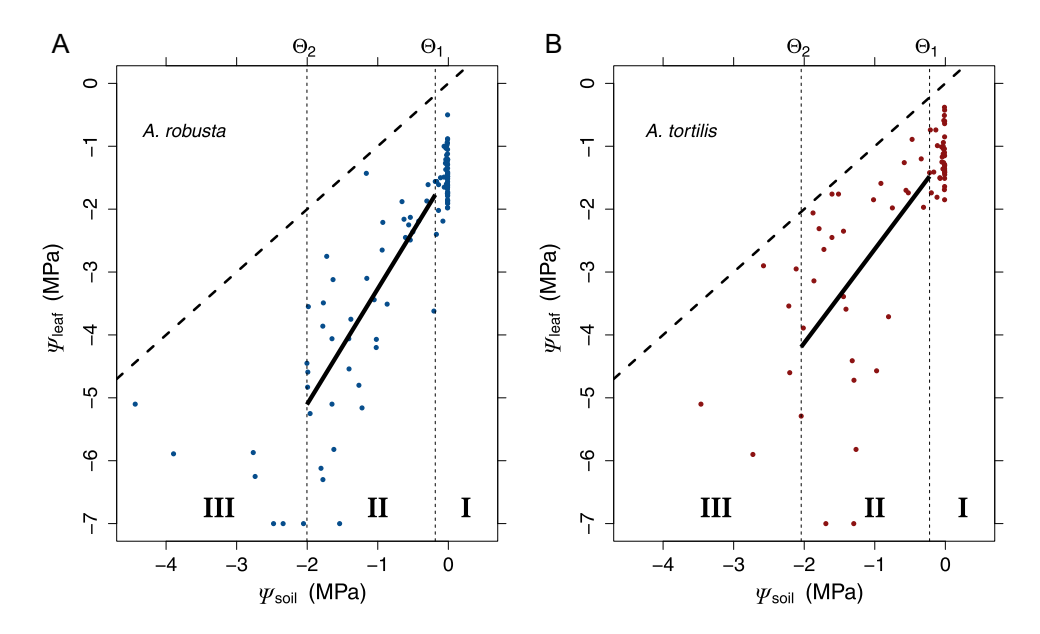


FIGURE 3 Water potential curves showing the trajectory of leaf (Ψ_{leaf}) and soil water potentials (Ψ_{soil}) during the drought for (A) *Acacia robusta* and (B) *A. tortilis*. Dashed vertical lines represent the transition points (Θ_1 and Θ_2) between Phases I-II and II-III. Thick dashed line is the 1:1 relationship between Ψ_{leaf} and Ψ_{soil} . Thick solid lines are the linear regression in Phase II. Initially in Phase I, Ψ_{leaf} fluctuated largely independently of Ψ_{soil} . After Θ_1 , lack of stomatal closure affected the Ψ_{leaf}/Ψ_{soil} relationship of Phase II, with Ψ_{leaf} declining faster than the declines in Ψ_{soil} indicating extreme anisohydry. Beyond Θ_2 , Ψ_{leaf} and Ψ_{soil} were effectively uncoupled in Phase III.

considered statistically nonsignificant due to the overlapping 95% confidence intervals (Table 1).

We also conducted an additional analysis of PLC data as categorical data, rather than continuous values of Ψ_{leaf} by discretizing the PLC data into bins of Ψ_{leaf} (Appendix S4). This approach provides a simple between-species comparison of PLC within important ranges of Ψ_{leaf} that would elucidate potential overfitting of our vulnerability curve models. This additional analysis also showed that PLC did not differ between species within each bin, further supporting our conclusion that the species do not differ in their hydraulic vulnerability.

DISCUSSION

We initially hypothesized that *Acacia* FYS in seasonally dry environments such as the Serengeti would invest in strategies to compete with grasses for water during pulses of resource availability. We expected both species to demonstrate relatively anisohydric stomatal behavior and to sustain hydraulic conductance even after water is withheld to compete with grasses after pulses of rainfall. Given that *A. tortilis* is widely distributed and more abundant in arid regions compared to *A. robusta*, we also predicted that *A. tortilis* would have a lower (=more negative) P_{50} and P_{88} , thus prolonging C gain during drought.

Our data show that both species are strongly anisohydric "water-spenders," yielding rapid carbon gain after pulses of moisture availability. Despite their comparable stomatal responses to declining soil moisture and similar whole-plant hydraulic vulnerability, they differed in their *rate* and *timing*

of water use, particularly at moderate levels of drought. *Acacia tortilis* transpires and depletes soil moisture faster than *A. robusta*, despite being equally vulnerable to declines in K_{plant} . In our experiment, this higher E of A. *tortilis* was the primary driver of the faster decline in its Ψ_{soil} and Ψ_{leaf} . During wet periods, its greater g_s and K_{max} allowed for this higher E, which ultimately led to greater A_{net} than for A. *robusta* when soil moisture was still high. However, the drawback of this greater E in A. *tortilis* was that soil moisture was "spent" much faster than for A. *robusta*, leading to an earlier cessation of gas exchange.

This difference between the species in their timing of water-use parallels the temporal trends in soil moisture after pulses of rainfall in the field. When we investigated the patterns of $\Psi_{\rm soil}$ in sites where these species occur, we found that the periods (number of days) of water availability are shorter (and less frequent) in sites where A. tortilis is more abundant (Appendix S4). Previous work has shown that $A_{\rm net}$ is strongly related to savanna tree seedlings' competitive ability against grasses (Campbell and Holdo, 2017), suggesting that a strategy like this—which maximizes $K_{\rm max}$ and $A_{\rm net}$ after pulses of water availability—is a particularly adaptive trait for A. tortilis. To our knowledge, this is the first time that physiological measurements at the leaf level (i.e., E) have been linked to species abundance and the rate of decline in $\Psi_{\rm soil}$ in African savannas.

Despite differences in the timing of soil drying and stomatal closure, both species demonstrated similar extreme anisohydric behavior as $\Psi_{\rm soil}$ declined. In phase II of the WP Curves (Figure 3), both species had a slope greater than 1, indicating that tension continues to increase as $\Psi_{\rm soil}$ declines (Martínez-Vilalta et al., 2014; Meinzer et al., 2016; Wu

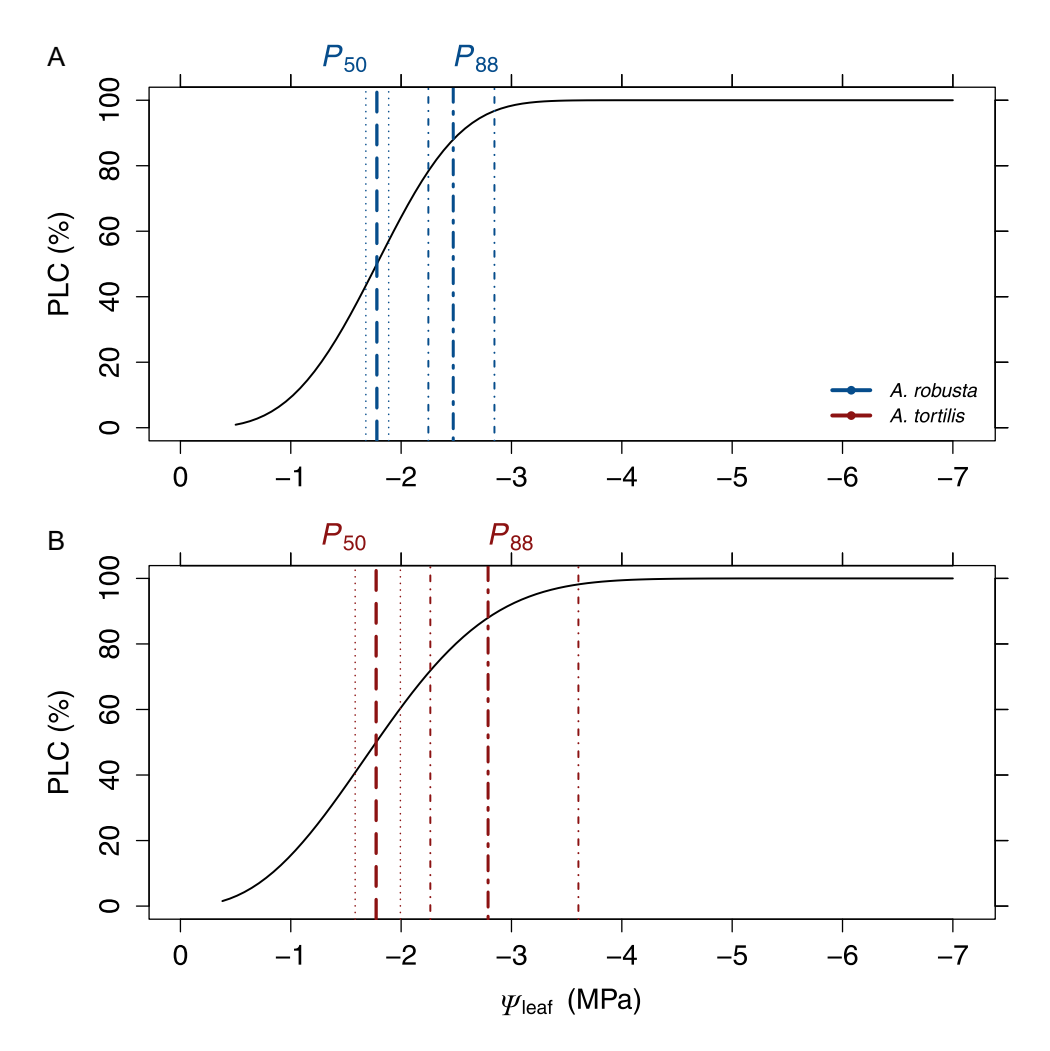


FIGURE 4 Vulnerability curves and estimates of leaf water potential (Y_{leaf}) required to induce a 50% (dashed line) and 88% (dash-dotted line) loss in whole-plant hydraulic conductance (P_{50} and P_{88} , respectively). *Acacia robusta* (A) and *A. tortilis* (B) did not differ in their hydraulic vulnerability. Solid black lines are the Weibull model for each species. Pairs of thin vertical lines on either side of P_{50} or P_{88} represent the 95% confidence intervals.

TABLE 1 Vulnerability curve parameter estimates and confidence intervals of Acacia tortilis and A. robusta.

P_x , S_x	Species	P_x estimate (MPa)	95% CI	S_x estimate	95% CI
P_{50}	A. robusta	-1.78	-1.68 to -1.89	66.27	47.65-88.96
	A. tortilis	-1.77	−1.58 to −1.99	48.30	31.38-80.21
P_{88}	A. robusta	-2.47	-2.25 to -2.85	35.03	22.29-51.11
	A. tortilis	-2.79	-2.26 to -3.61	22.56	11.67-44.59

Notes: P_{x0} leaf water potential (V_{leaf} MPa) required to induce a 50 or 88% decline in hydraulic conductance (K_{plant}); S_{x0} slope of the vulnerability curve at P_{50} or P_{88} .

et al., 2021). This steep slope implies that stomata were relatively insensitive to declining plant water status and that other mechanisms such as xylem embolism may be driving the drop in K_{plant} .

This anisohydric behavior has been observed in other arid and semi-arid ecosystems that experience pulses of water availability (Fu and Meinzer, 2018). In a similar drought experiment, Wujeska-Klause et al. (2015) compared seedlings of two *Acacia* species from contrasting habitats: *A. aneura* (arid habitats) and *A. melanoxylon*

(humid, less-arid habitats). They found anisohydric behavior in A. aneura, which had higher g_s during well-watered periods, but experienced sharper declines after the onset of drought, similarly to A. tortilis in our study. These differences between species mirror our inference that tree seedlings in arid habitats experience greater selection for maximizing gas exchange immediately after pulses of water availability, but at the expense of earlier cessation of C gain.

Vulnerability of K_{plant} to declining Ψ_{leaf} and Ψ_{soil} is an important metric of water-use strategies because it

integrates hydraulic conductance through multiple potential resistors: water uptake from soil into fine roots, through coarse roots, shoots, and leaves, and ultimately through stomata. During drought, declines in conductance of this hydraulic pathway are typically thought to be driven by excessive tension in xylem conduits, resulting in embolism (Tyree and Zimmermann, 2002). While failure of xylem function is a key mechanism limiting conductance in roots and stems, other mechanisms may simultaneously limit K_{plant} during drought. For example, drops in K_{plant} could be driven by declines in conductance from soil to the fine roots. Their minimal rooting volume exposes FYS to steep gradients of water potential in the rhizosphere, particularly in very dry soils (which Acacia FYS experience in the field), effectively uncoupling water content near the roots from the bulk soil water content (Carminati and Javaux, 2020).

Leaves themselves potentially limit K_{plant} due to embolism in leaf veins (Milburn, 1966) and stomatal closure, but also by declines in conductance of non-xylem pathways (Scoffoni et al., 2017). Water is transported into leaves via xylem, but must then pass through multiple tissues including vascular parenchyma and mesophyll before evaporating through stomatal pores. During drought, leaf shrinkage physically alters the non-xylem hydraulic pathway through leaves, which increases hydraulic resistance (Scoffoni et al., 2014). Leaf conductance may also be limited by membrane permeability, which declines during drought due to reduced aquaporin activity (Sack and Holbrook, 2006; Maurel et al., 2015). Regardless of which resistor is the primary driver of declining hydraulic conductance, the outcome for FYS's is the same: reduced capacity for gas exchange and increased probability of

Both of these species are drought-deciduous, which may be an additional mechanism by which savanna FYS's can avoid lethal desiccation. Our study plants dropped their leaves at extreme levels of drought (when Ψ_{leaf} reached ~ -5 MPa), but otherwise appeared to be alive. The potential advantage of this strategy is that it reduces transpiration and resource utilization during extended periods of drought, which may protect other tissues (stems and roots) from dehydration (Santiago et al., 2016). However, a strategy of drought deciduousness also limits the ability of FYS to take advantage of pulses of water, since some time is required for rehydration and production of new leaves. Although we did not directly measure their drought recovery after a pulse of water, anecdotally, we have observed leafless FYS (~6 months without water in our glasshouse) produce new leaves within days of re-watering. This ability to recover after re-watering suggests that the ability to tolerate long periods of dormancy during the dry season—but to rapidly produce new leaves and resume photosynthesis after a pulse of water-may play a critical role in the survival of these FYS's.

Our method of constructing whole-plant vulnerability curves and describing stomatal responses to drought is not without drawbacks. We used measurements of $\Psi_{\rm soil}$ to construct WP curves, rather than its more common proxy, $\Psi_{\rm predawn}$. Even though $\Psi_{\rm soil}$ more accurately reflects the maximum Ψ available to the plant (Hochberg et al., 2018), it is rarely measured directly. We attempted to verify that predawn $\Psi_{\rm leaf}$ is approximately equivalent with our measurements of $\Psi_{\rm soil}$, but this approach still assumes that $\Psi_{\rm soil}$ is homogenous throughout the rooting volume and that soil hydraulic continuity is sufficient (Donovan et al., 2001). Any potential error in $\Psi_{\rm soil}$ measurements, as well as inherent uncertainty in gas exchange and $\Psi_{\rm leaf}$ measurements, would ultimately be reflected in our calculated $K_{\rm plant}$ values.

CONCLUSIONS

With two tree species distributed on opposite ends of a precipitation and grass productivity gradient in a seasonally dry ecosystem, this study system is a valuable model for studying the mechanisms affecting FYS-grass competition. Both species maximize C gain during pulses of resource availability, which is likely stored belowground as nonstructural carbohydrates. During the dry season, a seedling with stored nonstructural carbohydrates can afford to lose aboveground tissues, whether it be through desiccation, senescence and drought deciduousness, fire, or herbivory, and then resume growth and/or resprout when precipitation returns. This ability to regenerate aboveground tissues and the high frequency of topkill and resprouting in this biome suggest that FYS establishment in savannas is, at least in part, dependent upon growing as fast as possible to establish belowground biomass from which a seedling can resprout after disturbance. Thus, competition with "water-spender" grasses (Williams et al., 1998) causes strong natural selection against FYS that cannot gain enough carbon and store it belowground (the so-called "Gulliver syndrome" sensu Bond and van Wilgen, 1996). Although we only compared two species here, hydraulic traits may play a similarly important role in seedling establishment of other savanna species that experience strong competition with grasses. Our study provides important insight into the role of water-use strategies and hydraulic traits in FYS survival and, ultimately, about the mechanisms enabling the tree-grass coexistence observed in savannas.

AUTHOR CONTRIBUTIONS

S.T.C. designed the study, collected and analyzed the data, and wrote the manuscript. T.M.A. collected field data in the Serengeti. T.M.A. and W.K.S. contributed data interpretation and manuscript revisions.

ACKNOWLEDGMENTS

The authors thank Caleb BrabbleRose for assistance with data collection. Funding was provided by Vecellio Fund at Wake Forest University to S.T.C., WFU Department of Biology, Reynolds-Babcock Fund to W.K.S., and National

Science Foundation (BCS-1461728) to T.M.A. We are grateful to the anonymous reviewers; their feedback greatly improved the manuscript.

DATA AVAILABILITY STATEMENT

The data that support the findings of this study are available from the Dryad Digital Repository: https://doi.org/10.5061/dryad.7h44j0zwx (Cory, 2022).

ORCID

Scott T. Cory http://orcid.org/0000-0002-3103-0988

REFERENCES

- Anderson, T. M., J. Dempewolf, K. L. Metzger, D. N. Reed, and S. Serneels. 2008. Generation and maintenance of heterogeneity in the Serengeti Ecosystem. *In A. R. E. Sinclair, C. Packer, S. A. R. Mduma, and J. M. Fryxell [eds.]*, Serengeti III: human impacts on ecosystem dynamics, 135–182. University of Chicago Press, Chicago, IL, USA.
- Anderson, T. M., T. Morrison, D. Rugemalila, and R. Holdo. 2015. Compositional decoupling of savanna canopy and understory tree communities in Serengeti. *Journal of Vegetation Science* 26: 385-394.
- Bond, W. J., and B. W. van Wilgen. 1996. Fire and plants. Chapman and Hall, London, UK.
- Brodersen, C. R., M. J. Germino, D. M. Johnson, K. Reinhardt, W. K. Smith, L. M. Resler, M. Y. Bader, et al. 2019. Seedling survival at timberline is critical to conifer mountain forest elevation and extent. Frontiers in Forests and Global Change 2: 1–12.
- Campbell, T. A., and R. M. Holdo. 2017. Competitive response of savanna tree seedlings to C_4 grasses is negatively related to photosynthesis rate. *Biotropica* 49: 774–777.
- Carminati, A., and M. Javaux. 2020. Soil rather than xylem vulnerability controls stomatal response to drought. *Trends in Plant Science* 25: 868–880.
- Chesson, P., R. L. E. Gebauer, S. Schwinning, N. Huntly, K. Wiegand, M. S. K. Ernest, A. Sher, et al. 2004. Resource pulses, species interactions, and diversity maintenance in arid and semi-arid environments. *Oecologia* 141: 236–253.
- Chidumayo, E. N. 2013. Effects of seed burial and fire on seedling and sapling recruitment, survival and growth of African savanna woody plant species. *Plant Ecology* 214: 103–114.
- Cory, S. 2022. Data from: first-year Acacia seedlings are anisohydric 'water-spenders' but differ in their rates of water use. *Dryad Digital Repository*. https://doi.org/10.5061/dryad.7h44j0zwx
- Cramer, M. D., S. B. M. Chimphango, A. Van Cauter, M. S. Waldram, and W. J. Bond. 2007. Grass competition induces N_2 fixation in some species of African Acacia. *Journal of Ecology* 95: 1123–1133.
- Crawley, M. J. 2007. The R book. John Wiley, Chichester, UK.
- Donovan, L., M. Linton, and J. Richards. 2001. Predawn plant water potential does not necessarily equilibrate with soil water potential under well-watered conditions. *Oecologia* 129: 328–335.
- Duursma, R., and B. Choat. 2017. fitplc—an R package to fit hydraulic vulnerability curves. *Journal of Plant Hydraulics* 4: e002.
- Dwyer, J. M., R. J. Fensham, R. J. Fairfax, and Y. M. Buckley. 2010. Neighbourhood effects influence drought-induced mortality of savanna trees in Australia. *Journal of Vegetation Science* 21: 573–585.
- February, E. C., S. I. Higgins, W. J. Bond, and L. Swemmer. 2013. Influence of competition and rainfall manipulation on the growth responses of savanna trees and grasses. *Ecology* 94: 1155–1164.
- Fu, X., and F. C. Meinzer. 2018. Metrics and proxies for stringency of regulation of plant water status (iso/anisohydry): a global data set reveals coordination and trade-offs among water transport traits. *Tree Physiology* 39: 122–134.
- Grossnickle, S. C. 2012. Why seedlings survive: influence of plant attributes. *New Forests* 43: 711–738.

- Hochberg, U., F. E. Rockwell, N. M. Holbrook, and H. Cochard. 2018. Iso/ anisohydry: a plant–environment interaction rather than a simple hydraulic trait. *Trends in Plant Science* 23: 112–120.
- Hoffmann, W. A., E. L. Geiger, S. G. Gotsch, D. R. Rossatto, L. C. R. Silva, O. L. Lau, M. Haridasan, and A. C. Franco. 2012. Ecological thresholds at the savanna–forest boundary: how plant traits, resources and fire govern the distribution of tropical biomes. *Ecology Letters* 15: 759–768.
- Holdo, R. M., T. M. Anderson, and T. Morrison. 2014. Precipitation, fire and demographic bottleneck dynamics in Serengeti tree populations. *Landscape Ecology* 29: 1613–1623.
- Holdo, R. M., D. A. Onderdonk, A. G. Barr, M. Mwita, and T. M. Anderson. 2020. Spatial transitions in tree cover are associated with soil hydrology, but not with grass biomass, fire frequency, or herbivore biomass in Serengeti savannahs. *Journal of Ecology* 108: 586–597.
- Johnson, D. M., K. A. McCulloh, and K. Reinhardt. 2011. The earliest stages of tree growth: development, physiology and impacts. *In F. C.* Meinzer [ed.], Size- and age-related changes in tree structure and function, 91–119. Springer, Dordrecht, Netherlands.
- Kambatuku, J. R., M. D. Cramer, and D. Ward. 2013. Overlap in soil water sources of savanna woody seedlings and grasses. *Ecohydrology* 6: 464-473
- Kannenberg, S. A., J. S. Guo, K. A. Novick, W. R. L. Anderegg, X. Feng, D. Kennedy, A. G. Konings, et al. 2021. Opportunities, challenges and pitfalls in characterizing plant water-use strategies. *Functional Ecology* 36(1): 24–37.
- Katabuchi, M. 2015. LeafArea: an R package for rapid digital image analysis of leaf area. Ecological Research 30: 1073–1077.
- Ketter, B. L., and R. M. Holdo. 2018. Strong competitive effects of African savanna C_4 grasses on tree seedlings do not support rooting differentiation. *Journal of Tropical Ecology* 34: 65–73.
- Knipfer, T., N. Bambach, M. Isabel Hernandez, M. K. Bartlett, G. Sinclair, F. Duong, D. A. Kluepfel, and A. J. McElrone. 2020. Predicting stomatal closure and turgor loss in woody plants using predawn and midday water potential. *Plant Physiology* 184: 881–894.
- Martínez-Vilalta, J., and N. Garcia-Forner. 2017. Water potential regulation, stomatal behaviour and hydraulic transport under drought: deconstructing the iso/anisohydric concept. *Plant Cell and Environment* 40: 962–976.
- Martínez-Vilalta, J., R. Poyatos, D. Aguadé, J. Retana, and M. Mencuccini. 2014. A new look at water transport regulation in plants. New Phytologist 204: 105–115.
- Maurel, C., Y. Boursiac, D. T. Luu, V. Santoni, Z. Shahzad, and L. Verdoucq. 2015. Aquaporins in plants. *Physiological Reviews* 95: 1321–1358.
- McDowell, N., W. T. Pockman, C. D. Allen, D. D. Breshears, N. Cobb, T. Kolb, J. Plaut, et al. 2008. Mechanisms of plant survival and mortality during drought: why do some plants survive while others succumb to drought? New Phytologist 178: 719–739.
- McNaughton, S. J. 1985. Ecology of a grazing ecosystem: the Serengeti. *Ecological Monographs* 55: 259–294.
- Meinzer, F. C., D. R. Woodruff, D. E. Marias, D. D. Smith, K. A. McCulloh, A. R. Howard, and A. L. Magedman. 2016. Mapping 'hydroscapes' along the iso- to anisohydric continuum of stomatal regulation of plant water status. *Ecology Letters* 19: 1343–1352.
- Midgley, J. J., M. J. Lawes, and S. Chamaillé-Jammes. 2010. Savanna woody plant dynamics: the role of fire and herbivory, separately and synergistically. *Australian Journal of Botany* 58: 1–11.
- Milburn, J. A. 1966. The conduction of sap—I. Water conduction and cavitation in water stressed leaves. *Planta* 69: 34–42.
- Morrison, T. A., R. M. Holdo, and T. M. Anderson. 2016. Elephant damage, not fire or rainfall, explains mortality of overstorey trees in Serengeti. *Journal of Ecology* 104: 409–418.
- Morrison, T. A., R. M. Holdo, D. M. Rugemalila, M. Nzunda, and T. M. Anderson. 2019. Grass competition overwhelms effects of herbivores and precipitation on early tree establishment in Serengeti. *Journal of Ecology* 107: 216–228.
- Nobel, P. S. 2009. Physiochemical and environmental plant physiology, 4th ed. Elsevier, Oxford, UK.

- Nolf, M., B. Beikircher, S. Rosner, A. Nolf, and S. Mayr. 2015. Xylem cavitation resistance can be estimated based on time-dependent rate of acoustic emissions. *New Phytologist* 208: 625–632.
- R Core Team. 2018. R: a language environment for statistical computing. R Foundation for Statistical Computing, Vienna, Austria. Website: https://www.r-project.org
- Rietkerk, M., F. van den Bosch, and J. van de Koppel. 1997. Site-specific properties and irreversible vegetation changes in semi-arid grazing systems. Oikos 80: 241–252.
- Rugemalila, D. M., T. M. Anderson, and R. M. Holdo. 2016. Precipitation and elephants, not fire, shape tree community composition in Serengeti National Park, Tanzania. *Biotropica* 48: 476–482.
- Rugemalila, D. M., S. T. Cory, W. K. Smith, and T. M. Anderson. 2020. The role of microsite sunlight environment on growth, architecture, and resource allocation in dominant *Acacia* tree seedlings, in Serengeti, East Africa. *Plant Ecology* 221: 1187–1199.
- Sack, L., and N. M. Holbrook. 2006. Leaf hydraulics. Annual Review of Plant Biology 57: 361–381.
- Sack, L., P. J. Melcher, M. A. Zwieniecki, and N. M. Holbrook. 2002. The hydraulic conductance of the angiosperm leaf lamina: a comparison of three measurement methods. *Journal of Experimental Botany* 53: 2177–2184
- Sankaran, M., N. Hanan, R. Scholes, J. Ratnam, D. Augustine, B. Cade, J. Gignoux, et al. 2005. Determinants of woody cover in African savannas. *Nature* 438: 846–849.
- Sankaran, M., J. Ratnam, and N. Hanan. 2008. Woody cover in African savannas: the role of resources, fire and herbivory. Global Ecology and Biogeography 17: 236–245.
- Santiago, L. S., D. Bonal, M. E. De Guzman, and E. Ávila-Lovera. 2016. Drought survival strategies of tropical trees. In G. Goldstein and L. S. Santiago [eds.], Tropical tree physiology: adaptations and responses in a changing environment, 243–258. Springer International, Cham, Switzerland.
- Scholes, R. J., and S. R. Archer. 1997. Tree-grass interactions in savannas.

 Annual Review of Ecology and Systematics 28: 517-544.
- Schwinning, S., and J. R. Ehleringer. 2001. Water use trade-offs and optimal adaptations to pulse-driven arid ecosystems. *Journal of Ecology* 89: 464–480
- Scoffoni, C., C. Albuquerque, C. R. Brodersen, S. V. Townes, G. P. John, M. K. Bartlett, T. N. Buckley, et al. 2017. Outside-xylem vulnerability, not xylem embolism, controls leaf hydraulic decline during dehydration. *Plant Physiology* 173: 1197–1210.
- Scoffoni, C., C. Vuong, S. Diep, H. Cochard, and L. Sack. 2014. Leaf shrinkage with dehydration: coordination with hydraulic vulnerability and drought tolerance. *Plant Physiology* 164: 1772–1788.
- Tardieu, F., and T. Simonneau. 1998. Variability among species of stomatal control under fluctuating soil water status and evaporative demand: modelling isohydric and anisohydric behaviours. *Journal of Experimental Botany* 49: 419–432.
- Tsuda, M., and M. T. Tyree. 1997. Whole-plant hydraulic resistance and vulnerability segmentation in *Acer saccharinum*. *Tree Physiology* 17: 351–357.
- Tyree, M. T., and M. H. Zimmermann. 2002. Xylem structure and the ascent of sap, 2nd ed. Springer, Berlin, Germany.

- Venturas, M. D., J. S. Sperry, and U. G. Hacke. 2017. Plant xylem hydraulics: what we understand, current research, and future challenges. *Journal of Integrative Plant Biology* 59: 356–389.
- Ward, D., and K. J. Esler. 2011. What are the effects of substrate and grass removal on recruitment of *Acacia mellifera* seedlings in a semi-arid environment? *Plant Ecology* 212: 245–250.
- Ward, D., K. Wiegand, and S. Getzin. 2013. Walter's two-layer hypothesis revisited: back to the roots! *Oecologia* 172: 617–630.
- Williams, K. J., B. J. Wilsey, S. J. Mcnaughton, and F. F. Banyikwa. 1998. Temporally variable rainfall does not limit yields of Serengeti grasses. Oikos 81: 463–470.
- Wu, G., K. Guan, Y. Li, K. A. Novick, X. Feng, N. G. McDowell, A. G. Konings, et al. 2021. Interannual variability of ecosystem iso/ anisohydry is regulated by environmental dryness. *New Phytologist* 229: 2562–2575.
- Wujeska-Klause, A., G. Bossinger, and M. Tausz. 2015. Seedlings of two *Acacia* species from contrasting habitats show different photoprotective and antioxidative responses to drought and heatwaves. *Annals of Forest Science* 72: 403–414.
- Xu, X., D. Medvigy, and I. Rodriguez-Iturbe. 2015. Relation between rainfall intensity and savanna tree abundance explained by water use strategies. Proceedings of the National Academy of Sciences, USA 112: 12992–12996.
- Yang, S., and M. T. Tyree. 1994. Hydraulic architecture of Acer saccharum and A. rubrum: comparison of branches to whole trees and the contribution of leaves to hydraulic resistance. Journal of Experimental Botany 45: 179–186.

SUPPORTING INFORMATION

Additional supporting information may be found online in the Supporting Information section at the end of the article.

Appendix S1. Diagram of whole-plant hydraulic conductance (K_{plant}) measurements.

Appendix S2. Species distributions and field Ψ_{soil} .

Appendix S3. Equilibrium of predawn Ψ_{leaf} and Ψ_{soil} from the Ψ_{soil} -sensor validation experiment.

Appendix S4. Categorical analysis of vulnerability curves.

How to cite this article: Cory, S. T., W. K. Smith, and T. M. Anderson. 2022. First-year *Acacia* seedlings are anisohydric "water-spenders" but differ in their rates of water use. *American Journal of Botany* 109(8): 1251–1261 https://doi.org/10.1002/ajb2.16032